CORE DESCRIPTION, INTERPRETATION, AND SEISMIC STRATIGRAPHY OF THE NANUSHUK AND TOROK FORMATIONS IN THE J.W. DALTON WELL, NORTH SLOPE, ALASKA

Joshua H. Long

Preliminary Interpretive Report 2025-7

Core depth 4697 ft, Nanushuk Formation. Imbricated, iron-cemented mudstone rip-up-clasts in fine- to medium-grained sandstone

2025
STATE OF ALASKA
DEPARTMENT OF NATURAL RESOURCES
DIVISION OF GEOLOGICAL & GEOPHYSICAL SURVEYS

STATE OF ALASKA
Mike Dunleavy, Governor

DEPARTMENT OF NATURAL RESOURCES
John Crowther, Commissioner-Designee

DIVISION OF GEOLOGICAL & GEOPHYSICAL SURVEYS
Erin Campbell, State Geologist & Director

Publications produced by the Division of Geological & Geophysical Surveys are available to download from the DGGS website (dggs.alaska.gov). Publications on hard-copy or digital media can be examined or purchased in the Fairbanks office:

Alaska Division of Geological & Geophysical Surveys (DGGS)
3354 College Road | Fairbanks, Alaska 99709-3707
Phone: 907.451.5010 | Fax 907.451.5050
dggspubs@alaska.gov | dggs.alaska.gov

DGGS publications are also available at:

Alaska State Library, Historical
Collections & Talking Book Center
395 Whittier Street
Juneau, Alaska 99801

Alaska Resource Library and
Information Services (ARLIS)
3150 C Street, Suite 100
Anchorage, Alaska 99503

Suggested citation:
Long, J.H., 2025, Core description, interpretation, and seismic stratigraphy of the Nanushuk and Torok formations in the J.W. Dalton well, North Slope, Alaska: Alaska Division of Geological & Geophysical Surveys Preliminary Interpretive Report 2025-7, 19 p., 1 sheet. https://doi.org/10.14509/31751

CORE DESCRIPTION, INTERPRETATION, AND SEISMIC STRATIGRAPHY OF THE NANUSHUK AND TOROK FORMATIONS IN THE J.W. DALTON WELL, NORTH SLOPE, ALASKA

Joshua H. Long[1]

INTRODUCTION

Legacy cores recovered during early oil and gas exploration efforts on Alaska's North Slope can provide valuable geological information for current and future subsurface evaluations and research efforts. LePain and Helmold (2021) presented detailed core descriptions and interpretations of the Nanushuk Formation from cores recovered from wells in the National Petroleum Reserve-Alaska (NPRA) and on state lands. However, several other wells, including J.W. Dalton, recovered relatively short cores from both the Nanushuk and Torok formations, which can provide valuable additional insight into the reservoir quality, sedimentology, and stratigraphy of these important oil and gas reservoirs. The core descriptions, facies interpretations, and seismic stratigraphy presented here for the Nanushuk and Torok formations in the J.W. Dalton well incorporate 2D and 3D seismic, paleontological, and petrological data. The purpose of this report is to discuss the data that are currently available for this well and present a basic stratigraphic and sedimentological context for the cored intervals of the Nanushuk and Torok formations. Supplemental photographs and data are available from the DGGS website at https://doi.org/10.14509/31751 and from the DGGS photo database https://maps.dggs.alaska.gov/photodb/#sort=filename%20asc&show=96&search=PIR%2B2025-7

WELL HISTORY AND DATA

The J.W. Dalton well was drilled near Alaska's Beaufort Sea coast in the northeastern part of the NPRA (fig. 1, 70.920496° N, 153.137527° W) in 1979 by Husky Oil NPR Operations Inc. and the U.S. Geological Survey (USGS) to a total depth of 9,367 feet. The target of the well was potential oil and gas reservoirs in the Lower Cretaceous Kuparuk and Triassic Ivishak formations, as well as the Mississippian Lisburne Group (Haywood and Legg, 1983). No economic hydrocarbons were recovered during five drill stem tests in the Ivishak Formation and Lisburne Group, and the well was subsequently plugged and abandoned (AOGCC, 2014).

Conventional cores (2 in diameter) were recovered from the Lower Cretaceous Nanushuk (57 ft) and Torok (31.3 ft) formations, the informally named pebble shale unit (Molenaar, 1983) (8.6 ft), the Ivishak Formation (208 ft), the Lisburne Group (53 ft), and from Ordovician-Silurian argillaceous metasedimentary basement rocks (AOGCC, 2014; Dumoulin, 2001).

The descriptions and interpretations of cores are integrated here with publicly available data sets including borehole geophysical logs (fig. 2 and sheet 1A- C; Zihlman and Oliver, 1999); NPRA 2D seismic data, which were collected between 1974–1981, reprocessed, and released in 2000 (Miller and others, 2000); the northeast NPRA 3D seismic survey which was acquired in 2006 and released as part of the State of Alaska's alternative tax credit for oil and gas program (https://dggs.alaska.gov/gmc/seismic-order.html); micropaleontological data (Mickey and others, 2006), and petrographic data (Pore Scale Solutions Ltd., and Santos Ltd., 2025). These data sets are supplemented by the well history from the Alaska Oil and Gas Conservation Commission (AOGCC, 2014) and a geological summary prepared by the USGS

[1]Alaska Division of Geological & Geophysical Surveys, 3354 College Road, Fairbanks, AK 99709

(Haywood and Legg, 1983). Cores from the J.W. Dalton well, discussed in this report, are part of the NPRA core collection archived at the Alaska Division of Geological & Geophysical Survey's Geologic Material Center in Anchorage, Alaska.

REGIONAL SETTING AND STRATIGRAPHY

The Colville foreland basin developed as a result of the collision of the Alaska microplate with a series of accreted terranes beginning in the middle to late Jurassic, with associated tectonic phases continuing into the present day (Grantz and others, 1994; O'Sullivan and others, 1994; Rollins and others, 2024). The roughly east-west trending Brooks Range orogenic belt, and the Barrow Arch, a basement-involved structural high which roughly parallels Alaska's arctic coast (fig. 1; see Homza and others [2020] for detailed discussion regarding the etymology and usage of this term) bound the Mesozoic–Cenozoic Colville foreland basin foredeep that accumulated 8-10 km of syn- and post-tectonic deposits (Houseknecht, 2019). North of the Barrow Arch, a complex, roughly shore-parallel system of basement-involved normal faults, referred to as the Hinge Line Fault Zone (Bird, 2001), developed during the late Jurassic and early Cretaceous, associated with the opening of the Canada Basin.

The non-marine, shallow-marine, and shelfal deposits of the Nanushuk Formation together with the shelfal, slope, and basin floor deposits of the Torok Formation form a series of large clinothems which prograded into the Colville Basin from both the west, with sediment derived from Mesozoic strata of the Chukotka Peninsula of present-day Russia, and from the south, with sediment derived from the Brooks Range (Mull and others, 2003; Houseknecht, 2019; Lease and others, 2022). In the subsurface, these depositional systems are defined by topset (Nanushuk Formation) and foreset and bottomset (Torok Formation) seismic geometries (fig. 3; Houseknecht and others, 2009).

Paleontological evidence indicates that the Nanushuk and Torok formations were deposited from the Aptian through the Cenomanian (Mull and others, 2003). Studies of foraminifera from the J.W. Dalton well suggest that Nanushuk and upper Torok Formation strata (2,760–5,610 ft measured depth [md]) at this location were deposited during the middle to late Albian in inner shelf to slope settings, and that lower Torok Formation strata (5,610–7,460 ft md) were deposited on the continental slope during the Aptian to early Albian (Mickey and others, 2006).

Historically, the Nanushuk Formation has produced hydrocarbons from relatively small pools (e.g., Qannik and Umiat), however, it has recently become the target of active exploration drilling along Alaska's North Slope, both in NPRA (Willow) and on state lands to the east and south (including Pikka Coyote, and Horseshoe) (fig. 1; Houseknecht and others, 2017). Deepwater sandstone reservoirs of the Torok Formation host hydrocarbon accumulations in the Moraine, Smith Bay, Nanuq, and Cassin oil pools (Bailey, 2016; Houseknecht and others, 2017; Houseknecht, 2019). The Nanushuk-Torok system hosts estimated combined mean volumes of 8.7 billion barrels of oil and 25 trillion cubic feet of recoverable gas, including potential recoverable estimates of 1.9–4.4 billion and 300 million barrels of oil from Pikka and Willow, respectively (Houseknecht and others, 2017; Sommer and others, 2021).

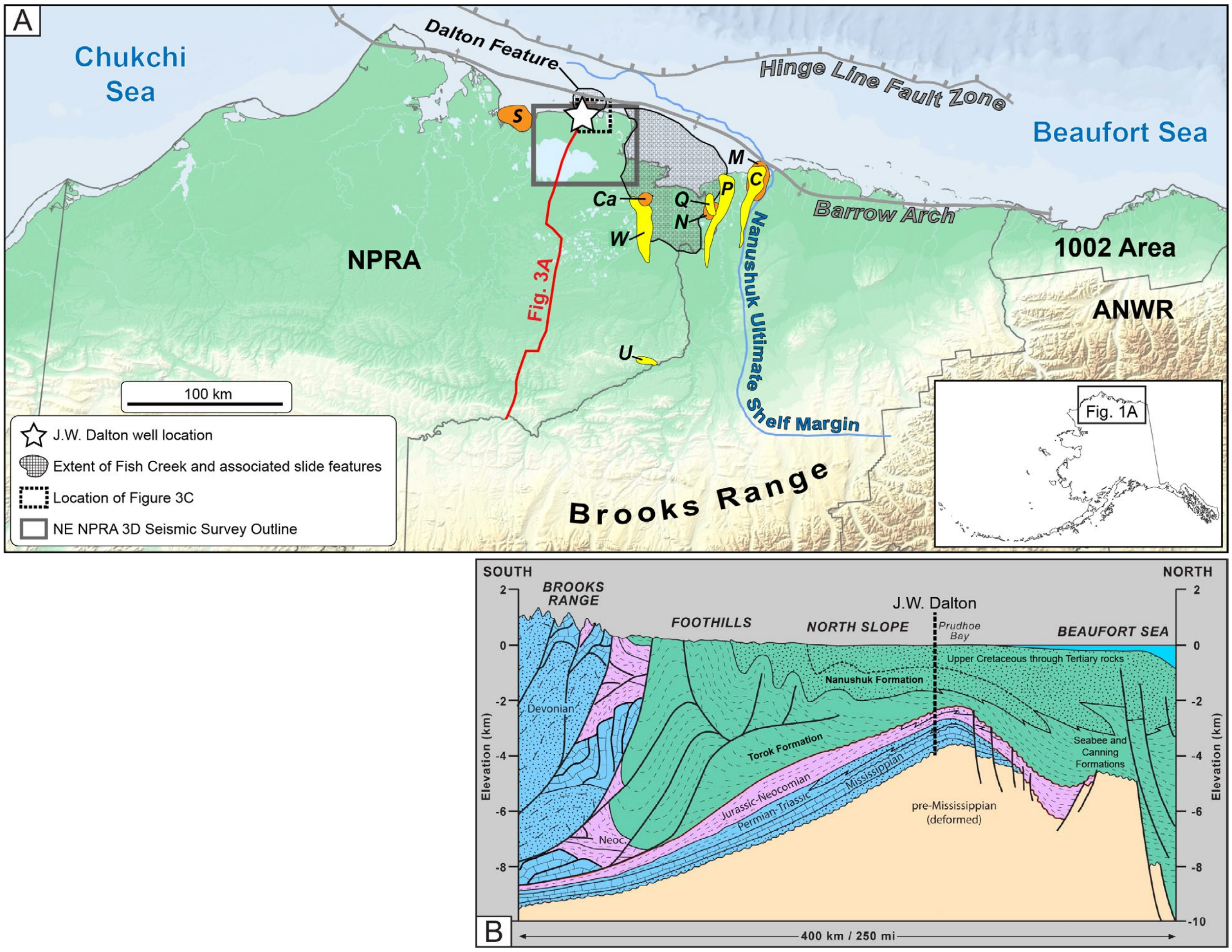

Figure 1. A. Map of study area showing relevant structural and stratigraphic elements. Hinge line fault zone and barrow arch from Bird (2001). Fish Creek Slide extent from Homza (2004). Dalton Feature from Weimer (1987). Nanushuk's ultimate shelf margin from Houseknecht (2019). Orange and yellow polygons show the locations of recent discoveries and existing oil pools in the Torok and Nanushuk formations, respectively. (S: Smith Bay, Ca: Cassin, N: Nanuq, M: Moraine, W: Willow, Q: Qannik, P: Pikka, C: Coyote, and U: Umiat). B. Generalized structural cross-section cartoon depicting the approximate location of the J.W. Dalton well relative to major tectonic elements of northern Alaska. Modified from Houseknecht and Bird (2011)

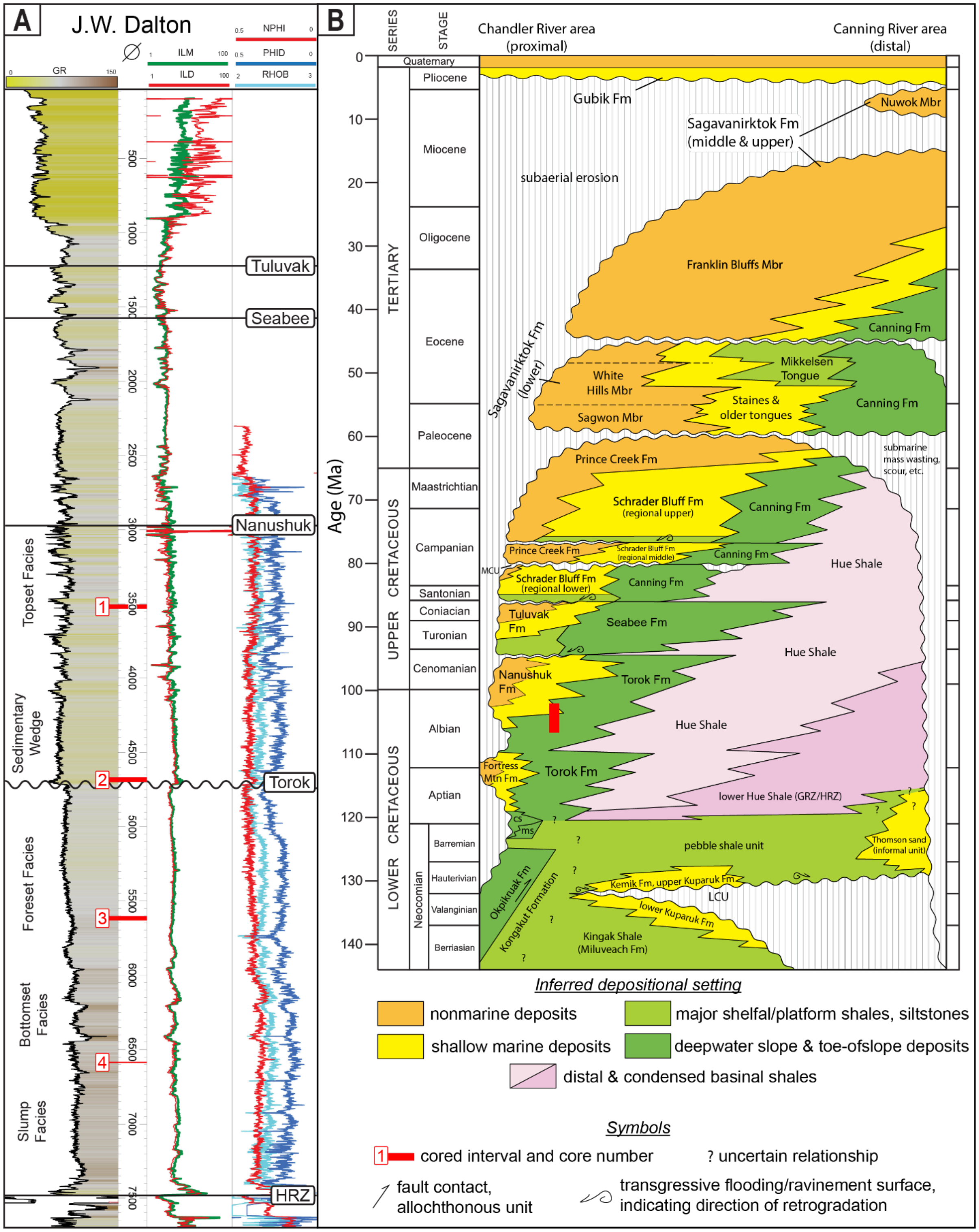

Figure 2. A. Petrophysical logs from the J.W. Dalton well, including gamma ray (GR, units are API units), resistivity [medium (ILM) and deep (ILD) induction logs, units are Ohm-meters], neutron porosity (NPHI, units are percent), density porosity (PHID, units are percent), and bulk density (RHOB, units are g/cm^3) logs, and are available from the USGS National Petroleum Reserve-Alaska Data Archive (National Petroleum Reserve-Alaska Data Archive). Formation tops based on the interpretation of seismic data and from Haywood (1983. Red numbers indicate cores included in this study. B. Stratigraphic column modified from Decker (2010) showing the age, simplified depositional settings, and stratigraphic relationships of Brookian strata in the central Colville basin.

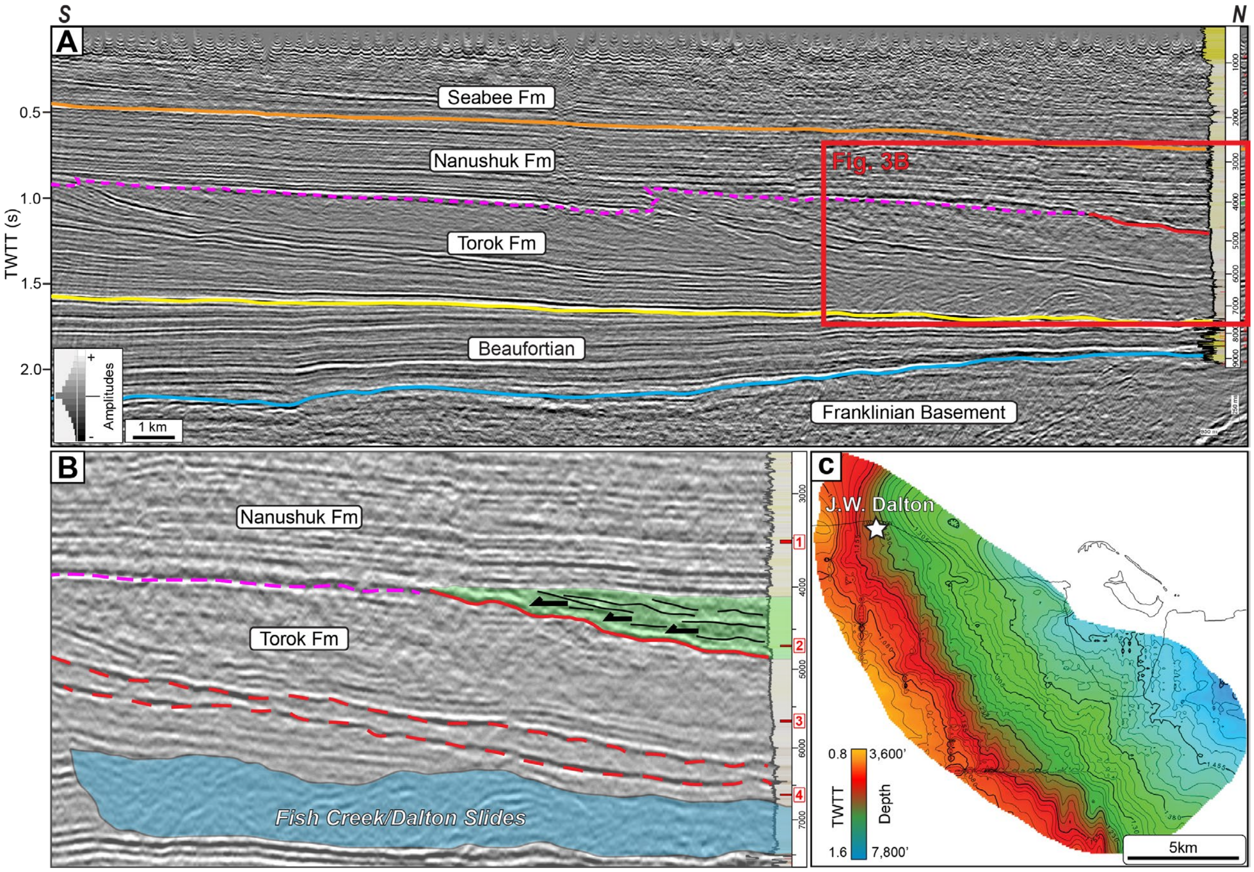

Figure 3. J.W. Dalton area seismic profiles. A. South-north regional 2D seismic line showing the generalized stratigraphy and associated seismic character of pre-Mississippian basement, Beaufortian, and lower Brookian strata. The left vertical axis shows two-way travel time (TWTT) in seconds; the right vertical axis shows the gamma-ray log for the J.W. Dalton well, with depth in feet. See figure 1 for the location. B. Detailed stratigraphic architecture of the Nanushuk and Torok formations related to the cored intervals discussed in this report. Dashed red lines indicate high-amplitude seismic reflectors that correlate to erosional or detachment surfaces within the Torok Formation. The solid red line marks the erosional base of the sedimentary wedge at the base of the Nanushuk Formation, with black arrows indicating onlapping seismic reflectors and black lines tracing progradational-to-aggradational surfaces within this wedge. The vertical axis on the right shows the gamma-ray log with depth in feet. Cored intervals and core numbers are indicated along the length of the wellbore in red. C. Time structure grid of the basal Nanushuk erosional surface. Estimated depths are based on the regional time-depth function presented by Grantz and May (1982).

CORE DESCRIPTIONS AND INTERPRETATIONS

Core Four: Torok Formation (6,585–6,589 ft)

Core four was recovered from a ~200-ft-thick interval exhibiting an overall decreasing-upwards gamma ray profile bound above and below by thin high gamma ray intervals (fig. 2A; sheet 1C). The cored interval lies within a thin zone of elevated gamma ray values (sheet 1C). The length of core four (4 ft) limits the available context for a detailed sedimentological interpretation.

Seismic Stratigraphy- Core four was recovered from lower foreset to proximal bottomset facies immediately above a widespread interval of slump deposits generally referred to as the Fish Creek Slides (figs. 2, 3A, and 3B). Weimer (1987) first defined what he referred to as the Dalton and Fish Creek features as isolated slumps and slides associated with mass transport of lower slope facies of the Torok Formation (fig. 1). Paleobathymetric lows created by the mounded morphology at the top of these features created localized accommodation for subsequent deepwater deposits of younger Torok Formation strata (Homza, 2004). These features are the result of detachment along the contact between the Torok Formation and the HRZ or Lower Cretaceous Unconformity (LCU) initiated by slip along underlying basement-involved faults (Homza, 2004).

Core Description- Core four consists primarily of very thin beds (< 3 cm) to thin laminae (< 0.3 cm) of massive mudstone, laminated mudstone, massive to weakly laminated siltstone, and very fine-grained sandstone (fig. 4A-D, sheet 1A). Sandstone ranges in thickness from thin laminae to very thin beds. It contains horizontal laminations (fig. 4A) and current-ripple cross-laminations (fig. 4B). Most sandstone beds have sharp bases, which commonly exhibit soft-sediment deformation and sharp upper contacts (figs. 4C and D). Massive mudstone beds contain contorted siltstone laminae and disseminated silt (fig. 4D).

Core Interpretation- The basinal setting, fine-grained nature, and dominance of lower flow regime and suspension deposits, including Bouma sequence components Tc, Td, and Te (Bouma, 1962), and combinations of these components, suggest deposition by low-density turbidity currents and from hemipelagic suspension (Lowe, 1982). Massive mudstones and silty mudstones were deposited by cohesive mudflows, potentially associated with low-density sediment gravity flows. The predominance of starved ripple cross-lamination suggests that, overall, sediment supply was low and that these structures are associated with traction deposition from dilute low-density turbidites or weak bottom currents.

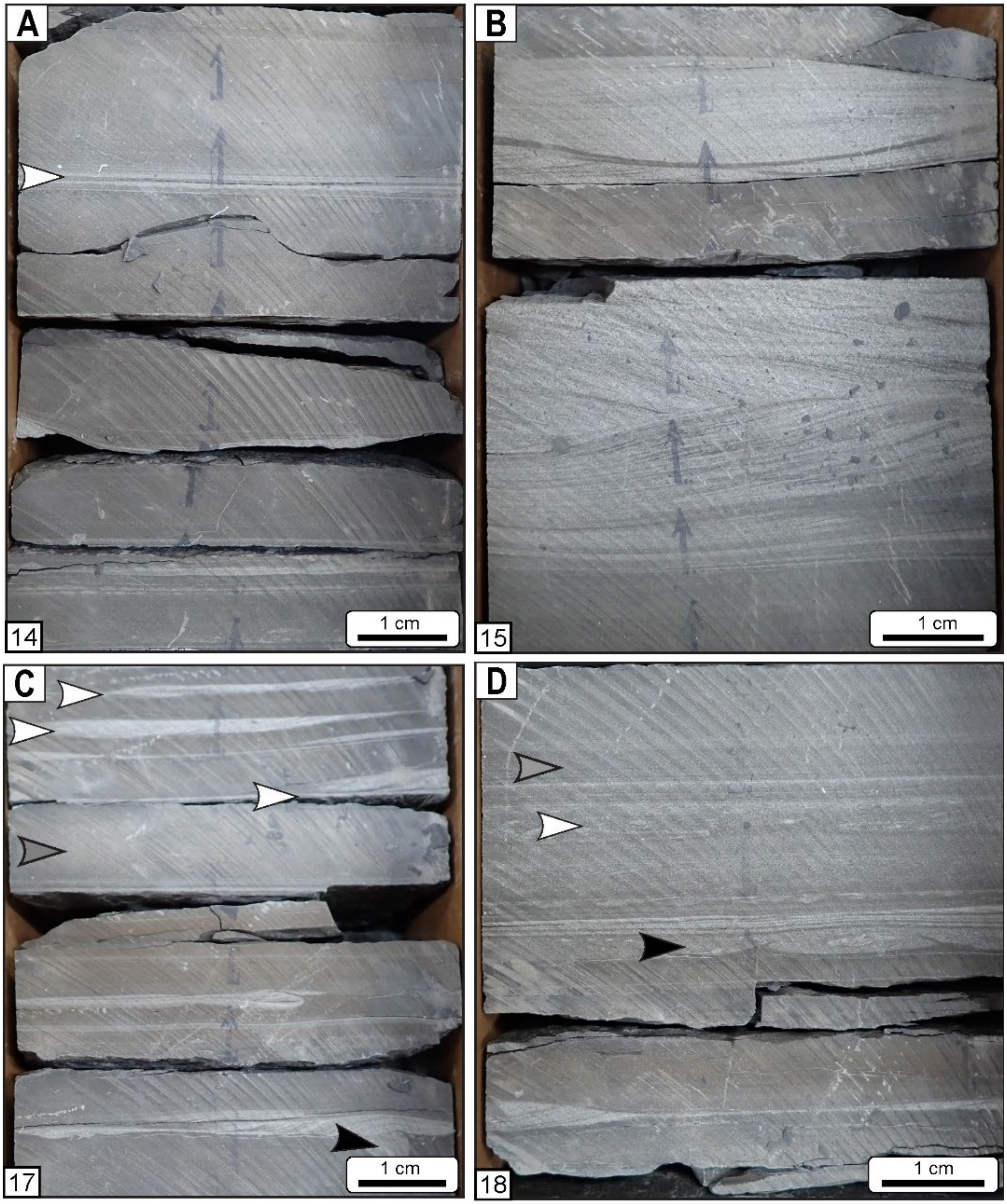

Figure 4. Detailed photographs of the Torok Formation in core four. A. Horizontal laminae of very fine-grained sandstone (white arrow). B. Beds of mud-draped, current ripple cross-laminations. C. Starved ripple cross-laminations (white arrows), soft-sediment deformation (black arrow), and massive mudstone (gray arrow). D. Contorted siltstone lamina and disseminated silt within a poorly sorted, massive bed (white arrow), load structures (black arrow), and interlaminated mudstone and siltstone (gray arrow). Numbers in the lower-left corners refer to photograph numbers, which are listed in the core description on sheet 1A. Cores are 2 inches wide.

Core Three: Torok Formation (5,603–5,630 ft)

Core three was recovered from a long interval of intermediate to high gamma-ray values (>75 API) that exhibit no obvious vertical trends (sheet 1C). Overall, the jagged gamma ray profile for the interval shown in sheet 1C suggests vertical aggradation of fine-grained heterolithic lithologies (Catuneanu, 2006).

Seismic Stratigraphy- Core three was recovered from low-amplitude, northerly to northeasterly dipping foresets (fig. 3B). The seismic reflectors that define this foreset interval are of moderate to low amplitude and mostly chaotic with a thin interval of basal undulatory, high-amplitude reflectors.

Core Description- Thin to thick (< 1 cm) laminae of dark gray mudstone, siltstone, and very fine-grained sandstone comprise the entirety of core three (sheet 1A, B; figs. 5A–C). Mudstone and siltstone laminae resemble those described for core four; however, laminae and thin sandstone beds are less abundant and generally thinner than those from core four. Sandstone laminae are very thin and commonly laterally discontinuous across the width of the core (fig. 5A), contain current ripple cross-laminations, and loaded basal contacts (fig. 5B–C). Mudstone laminae are thick and tend to lack internal bedding (figs. 5A–B).

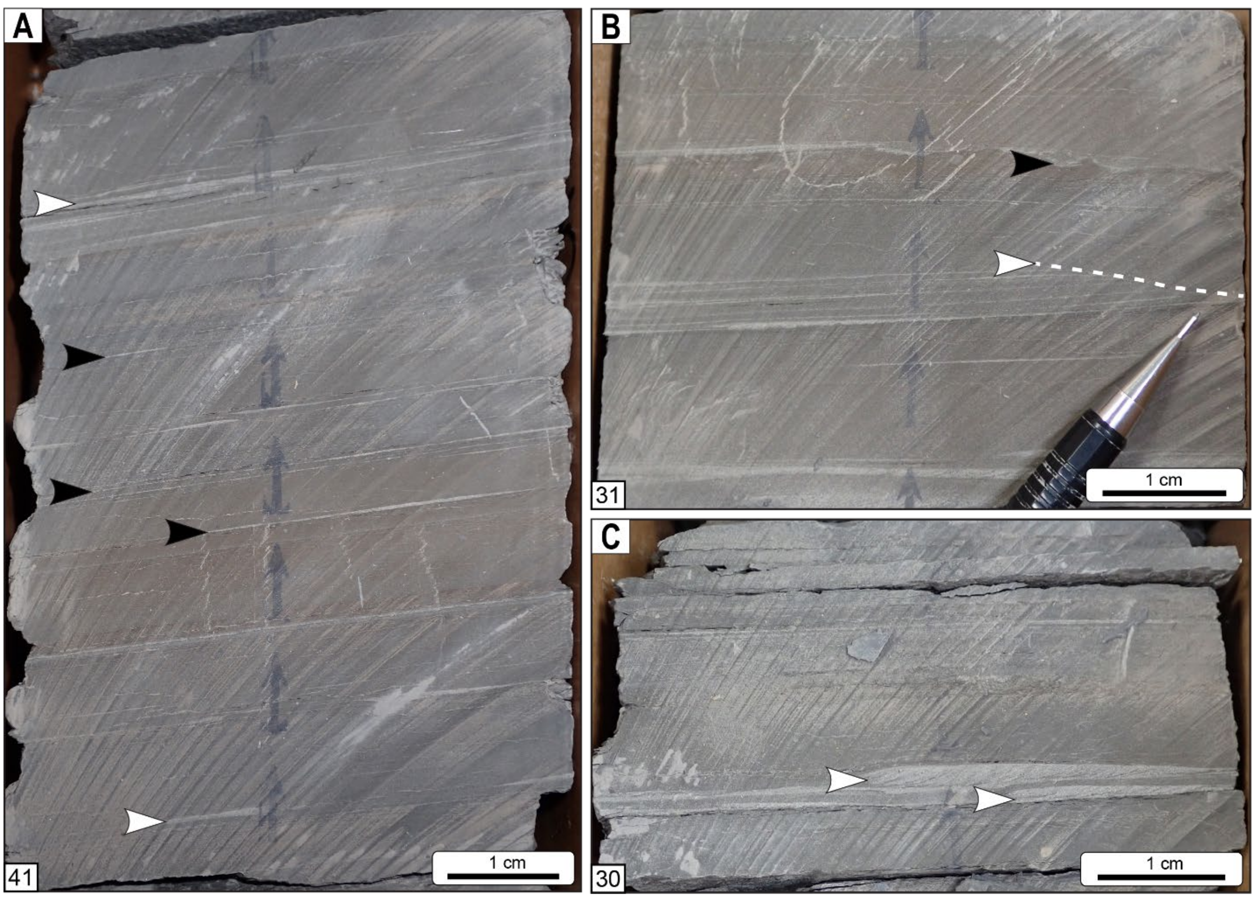

Figure 5. Detailed photographs of Torok Formation facies in core three. A. Thick laminae of dark gray massive mudstone and thin, discontinuous laminae of very fine-grained sandstone (black arrows). Some sandstone laminae preserve starved ripple cross-laminations (white arrows). B. Soft-sediment deformation (black arrow) and low-angle erosional surface (dashed white line). C. Sets of current ripple cross-laminae (white arrows). Numbers in the lower-left corners refer to photograph numbers, which are listed in the core description on sheet 1A. Cores are 2 inches wide.

Core Interpretation-Although the core three lacks the thicker sandstone beds that occur in core four, the overall interpretation of depositional facies is the same. Core three is dominated by very thinly bedded, very fine-grained sandstone and siltstone deposited by low-density turbidity currents and mudstone deposited from suspension of hemipelagic sediment. The relatively higher percentage of mudstone to coarser-grained sediments indicates an overall low-energy environment; however, truncated sandstone laminae (fig. 5B) attest to erosion by through-going sediment gravity flows or bottom currents. The low-density turbidites and hemipelagic sediments preserved in core three were deposited on the continental slope as part of a northeasterly prograding clinothem.

Core Two: Nanushuk Formation (4,667.1–4,692.7 ft)

Core two was recovered from an interval at the base of the Nanushuk Formation, which displays an overall increasing-upwards gamma ray profile (fig. 2). The relatively long length of core two, along with the excellent preservation of sedimentary structures, allows for a detailed description of this interval of the lower Nanushuk Formation. Five thin sections from core two were point-counted and summarized in Pore Scale Solutions Ltd., and Santos Ltd. (2025) (sheet 1A). These samples consist of well-sorted, lithic sandstones with mean grain sizes ranging from very fine lower (0.067 mm) to very fine upper (0.107 mm). They contain 50–57 percent rigid framework grains (quartz; feldspar; and plutonic, metamorphic and carbonate rock fragments), 41–50 percent ductile grains (intra- and extrabasinal rock fragments; micas; and detrital organic matter), and 0–1.5 percent authigenic material (siderite and clays) (Pore Scale Solutions Ltd., and Santos Ltd., 2025). Additionally, Bartsch-Winkler and Huffman (1988) reported petrographic data from two samples in the J.W. Dalton well, one in core one (3,524') and one in core two (4,687.5'). Most point-count categories differ between the two studies, making it difficult to compare or combine the datasets.

Seismic Stratigraphy- Core two was recovered from an interval immediately above an irregular, high-amplitude seismic reflector that truncates several underlying reflectors and is overlain by a series of low-angle, backstepping reflectors (fig. 3B). Small, low-angle progradational to aggradational reflectors downlap these onlapping reflectors and exhibit a toplap relationship with overlying topset reflectors (fig. 3B). The basal erosion surface and the toplap surface define a sedimentary wedge that pinches out to the southwest against the relict shelf margin; core two was taken from the base of this interval. Figure 3C shows a time-structure grid of the basal erosion surface derived from both 3D and 2D seismic data and defines a surface dipping to the northeast, roughly parallel to, but at a lower angle than, the dip of Torok Formation foresets in the area and exhibits roughly 2,100 ft of relief over the area that it was mapped (fig. 3C)

Core Description- Two basic lithofacies comprise the majority of the Nanushuk Formation in core two. These lithofacies are defined based on the relative abundances of sandstone and mudstone as either sandstone-rich (e.g., units 4, 9, and 15; sheet 1A) or mudstone-rich (e.g., units 5, 12, and 22; sheet 1A). The sedimentological and stratigraphic complexity of core two merits a more detailed discussion than do the other cores discussed in this report (figs. 6A-H).

Sandstone-rich units contain thin (3–10 cm) to very thin (1–3 cm) beds of fine lower- to fine upper-grained sandstone which display current ripple laminations, planar laminations, massive bedding, and disseminated carbonaceous material (fig. 6). The geometry of current ripple laminae is variable with intervals indicating a single dominant current direction (e.g., fig. 6D) as well as intervals indicating variable or bidirectional currents (e.g., fig. 6H). Tops of individual sandstone beds range from flat to undulatory (figs. 6B and E). Very thin beds to thick laminae of mudstone, carbonaceous mudstone, or organic material drape both the tops of sandstone beds as well as the foresets of ripple laminae within this lithofacies. Alternating beds and lamina of mudstone and/or carbonaceous material with sandstone form couplets which define evenly spaced, thinning upwards (fig. 6B), or thickening upwards (fig. 6H) bundles consistent with flaser, wavy, and lenticular bedding as defined by Reineck and Wunderlich (1968). Unit three (sheet 1A) is unique from other sandstone-rich units in core two in that it contains large, rounded spheroidal and as well as angular platy, generally bed-parallel, clasts of iron-cemented (siderite?) mudstone (fig. 6A). These mudstone clasts are rarely in contact with one another, instead, they are suspended within a matrix of massive, moderately well sorted, lower medium-grained sandstone.

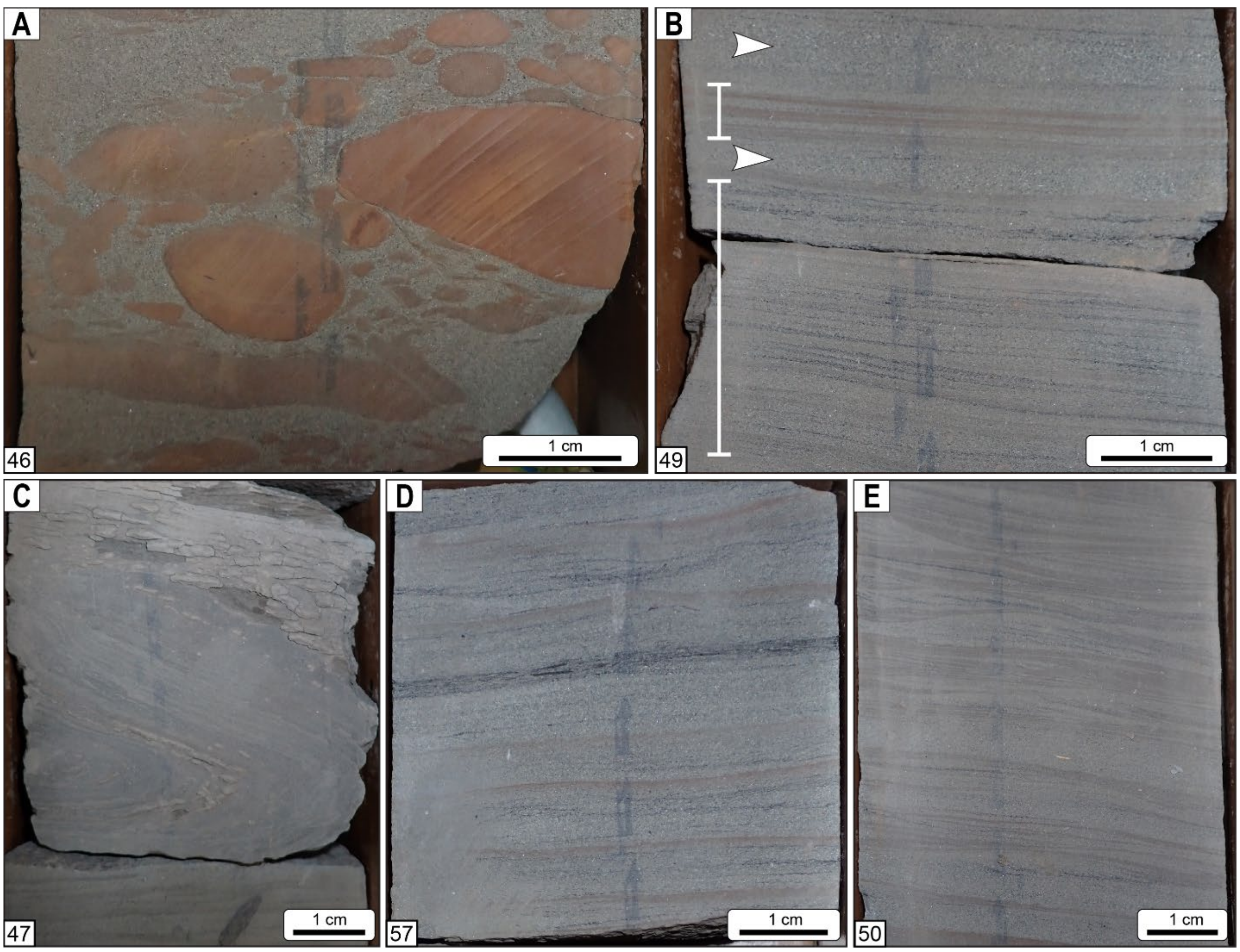

Figure 6. Detailed photographs of the Nanushuk Formation in core two. A. Angular and rounded sideritized mudstone rip-up-clasts from unit 3 (sheet 1A). B. Interbedded well-sorted, fine-grained sandstone, sideritized mudstone, and carbonaceous material in unit 4 (sheet 1A). C. Recumbent fold resulting from soft sediment deformation in unit 6 (sheet 1A). Vertical white lines mark rhythmic bedding intervals, defined by sandstone-mudstone/organic couplets. White arrows highlight relatively thicker massive or faintly ripple cross-laminated sandstone beds. D. Semi-regularly spaced ripple cross-laminated sandstone beds with foresets defined by organic drapes capped by thin sideritized mudstone caps. E. Very thin, mudstone-capped, ripple cross-laminated sandstone beds in unit 4 (sheet 1A).

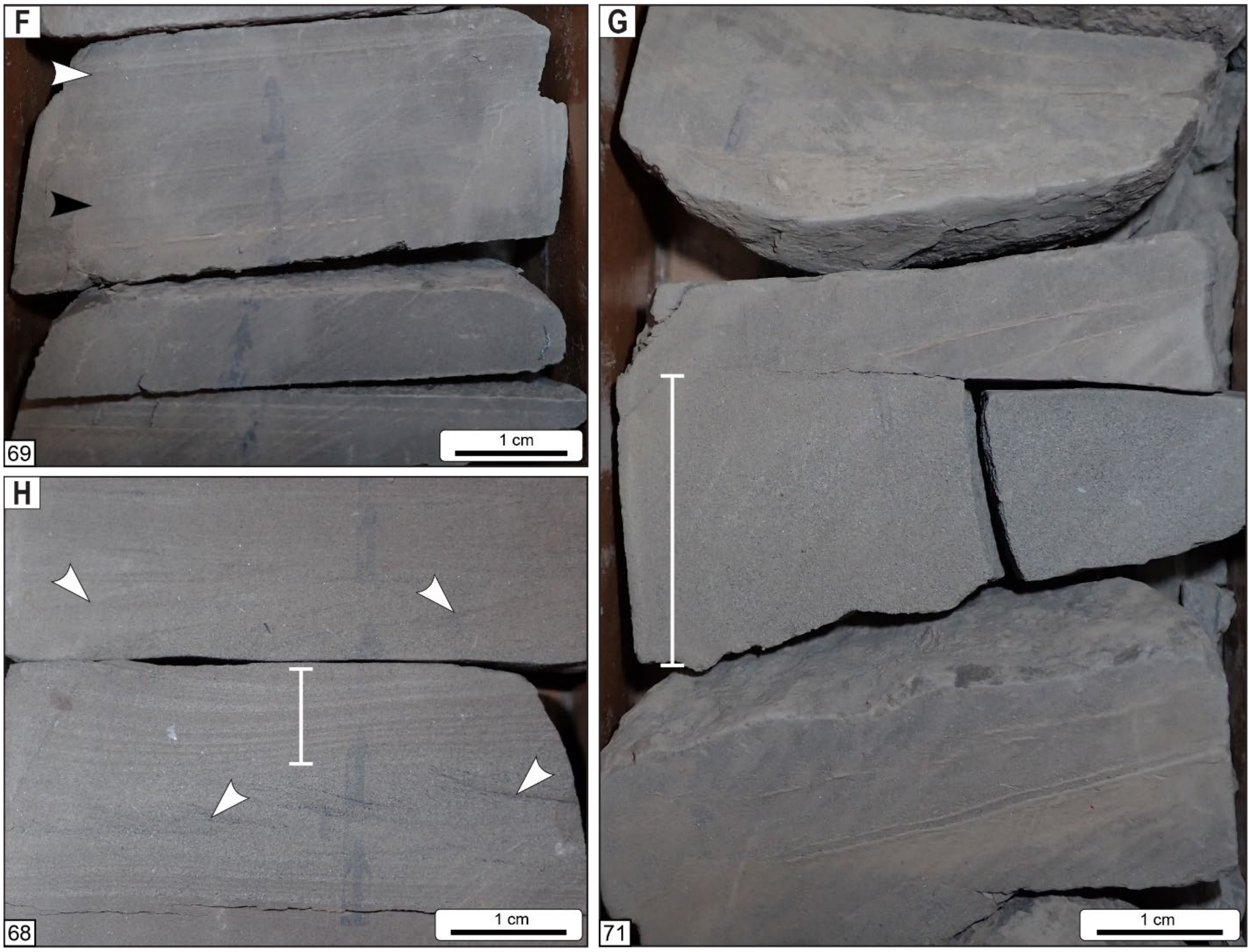

Figure 6. continued. Detailed photographs of the Nanushuk Formation in core two. F. Massive silty mudstone (black arrow) and thinly laminated silt and mudstone in unit 22 (sheet 1A). G. Wedge-shaped, massive, fine-grained sandstone (white bracket). H. Current ripple-laminations draped in carbonaceous detritus, indicating two dominant directions of transport (white arrows). Progressively thickening-upwards sandstone-mudstone couplets from unit 21 (vertical white line; sheet 1A). Numbers in the lower-left corners refer to photograph numbers, which are listed in the core description on sheet 1A. Cores are 2 inches wide.

Mudstone-rich lithofacies contain thin to very thin beds of massive mudstone and sandy mudstone with thin laminae of siltstone, as well as fine-grained and very fine-grained sandstone (figs. 6F and G). Sandstone laminae have sharp upper and lower contacts and are typically 2–3 mm thick. Thin sandstones exhibit current ripple cross-laminations or are structureless (i.e., massive). Aside from a single upper fine-grained sandstone bed at approximately 4,671 ft md, the upper 12 feet of core two is composed exclusively of this lithofacies (sheet 1A and 1B).

Core Interpretation- The dominance of high-frequency alternations of sandstone and mudstone in units 3–21 indicates variable, but persistent and potentially regular, fluctuations in hydrodynamic conditions. Thin, massive or ripple cross-laminated sandstone beds were deposited from suspension or by traction under lower flow regime conditions, respectively. Mudstones and detrital organic material were deposited by suspension in low-energy conditions as individual grains or as flocs (Flemming, 2011). The abundance of carbonaceous material indicates a source of detrital terrigenous plant material, and the presence of intraformational, angular, sideritized mudstone clasts suggests that this material has not been transported over a long distance but rather eroded from a proximal source.

The prevalence of sandstone-mudstone/organic couplets, multi-directional, and apparent bidirectional cross-laminae (fig. 6), support the interpretation that this section of the core was deposited under the influence of tides as rhythmites, cyclically stacked sand and mud lamina couplets whose thickness varies rhythmically (fig. 7A and B; Reineck and Singh,1973; Longhitano and others, 2012). Most current-generated structures suggest a dominant flow direction, a condition common even in tide-dominated environments where residual flow (net flow resulting from the interaction of fluvial, tide, and wave-generated currents) is largely a product of tidal asymmetry and river discharge (Goodbred and Saito, 2012). The thin sandstone beds in this section of the core lack indicators that would suggest overall waning flow conditions (i.e., fining-upwards grain size trends or Bouma-type successions), suggesting that the heterolithic deposits are not the product of sediment gravity flows; instead, they are the product of a roughly bimodal distribution of bottom current velocities. While undulatory tops of sandstone beds may suggest minor wave influence, the presence of combined flow ripples (fig. 6E) and sedimentary structures indicative of wave influence are rare, indicating either the setting is sheltered from wave energy or that in the vicinity of the J.W. Dalton well wave energy is generally weak.

The sedimentary structures present in the sandstone-rich vertical succession of units 3–21 define a transition from the high-energy conditions recorded in unit three, indicated by large intrabasinal clasts and coarser grain size, to carbonaceous-rich mixed-energy conditions of the overlying units, and are consistent with deposition in a tidally-influenced delta front setting (figs. 7C and D). More specifically, these are likely to represent the deposits of shallow distributary channels and tidal bars. In tide-dominated deltas, tidal bars are commonly associated with adjacent channels or gullies. They are dominated by heterolithic ripple cross-laminated facies including flaser-, wavy-, and lenticular-bedded very fine-grained sandstones, siltstones, and mudstones (Longhitano and others, 2012; Plink-Björklund, 2012). Similar barforms in modern and ancient tide-dominated delta-front settings commonly range in thickness from 5 to 10 m (Plink-Björklund, 2012).

A flooding surface at 4,679 ft separates the lower, sandstone-dominated, section of core two from the upper, mudstone-dominated section and may represent a phase of lobe abandonment, potentially as part of an ongoing transgression and backstepping of the deltaic or estuarine system; the latter interpretation is supported by the increasing-upwards gamma ray profile exhibited in the cored interval and the section immediately above (sheet 1C). Unit 22 (sheet 1A) generally lacks the rhythmic or regular arrangement of sandstone and mudstone beds, which are present in the underlying units. This change is consistent with the observation by Goodbred and Saito (2012) that tidal influence decreases basinward and may not be recognizable in mudstone-rich prodelta deposits. The subtle increase in grain size near the top of core two (sheet 1A) may be the result of an overlying phase of lobe progradation; however, given the abbreviated length of this interval, this interpretation is highly tentative. The general lack of recognizable biogenic structures throughout core two likely reflects elevated physicochemical stresses resulting from high sedimentation rates, fluctuations in salinity, substrate conditions, or a combination of these factors (Gingras and others, 2011).

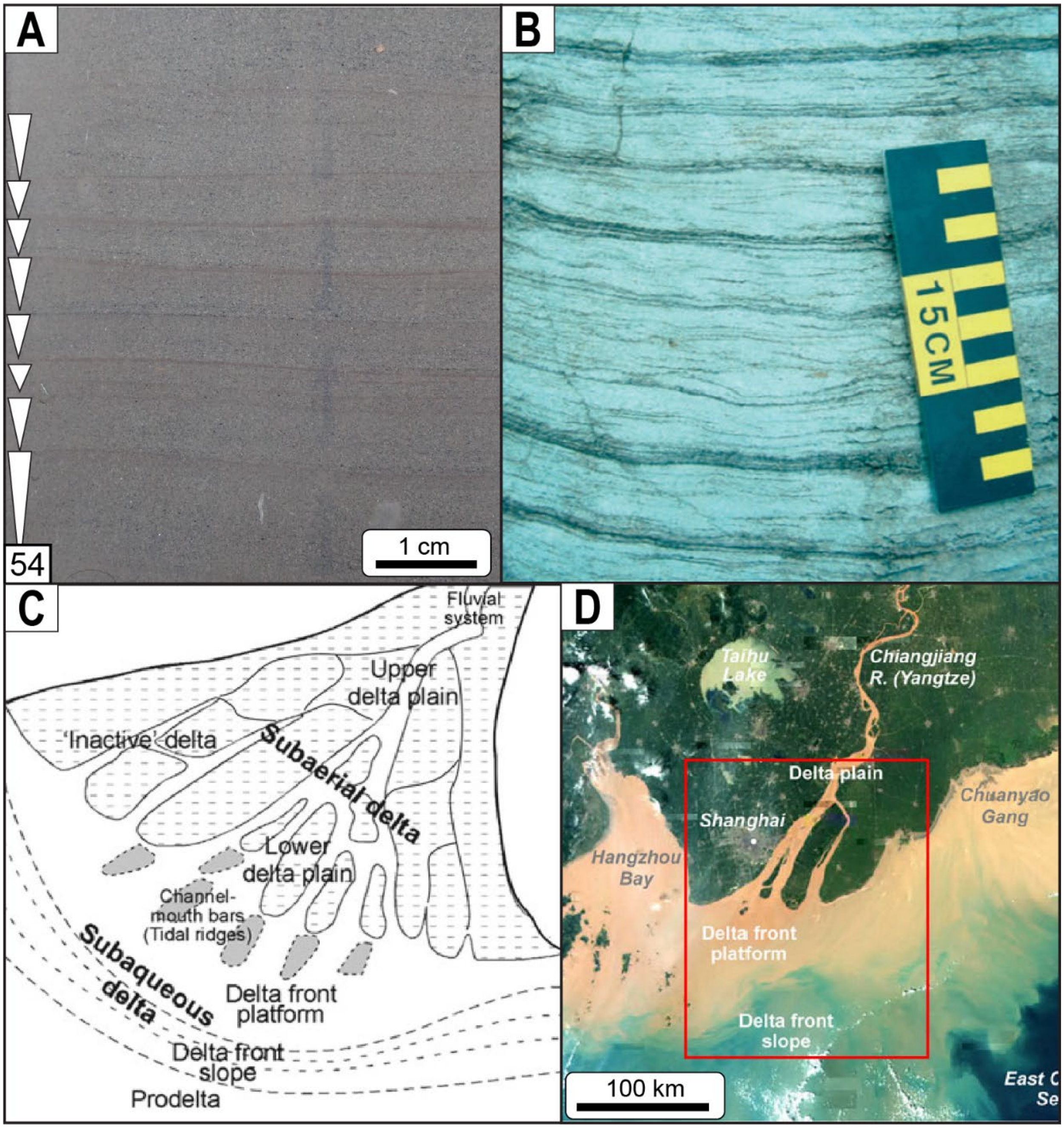

Figure 7. Tidally influenced facies and depositional analogues for the Nanushuk Formation in core two. A. Sandstone-mudstone couplets interpreted as tidal bundles or rhythmites from unit nine (sheet 1A) in core two. B. Example from Boyd and others (2006) of tidal rhythmites. C. Simplified depositional model for tide-dominated deltas. D. Modern tide-dominated delta, a potential analogue for the Nanushuk Formation in core two. The red box encompasses the Changjiang (Yangtze) River delta along China's east coast. Both C and D are from Goodbred and Saito (2012).

Core two was recovered from an overall fining-upward interval defined at its base by the sub-regional erosional surface evident in both seismic and well log data (sheet 1C and fig. 3). This erosional surface is interpreted as a sequence boundary that developed as a result of a significant fall in relative sea level and given its stratigraphic position, gravitational failure of shelf margin and upper slope deposits. The sequence boundary marks the base of a wedge of sediment consistent with what Posamentier and Allen (1993) referred to as a healing phase wedge. The basal section of the healing phase wedges typically preserves shallower water, relatively coarse-grained, tidally influenced deltaic deposits as components of the transgressive systems tract (Posamentier and Allen, 1993; Catuneanu, 2006). The broadly crescent-shaped morphology of the sequence boundary, as shown in fig. 3C, may have also served to amplify tidal resonance, a relationship discussed by Reynaud and Dalrymple (2012) related to scarps resulting from shelf margin failures.

Core One: Nanushuk Formation (3,503–3,530 ft)

The gamma-ray profile of the interval above the ore one contains several packages that exhibit pronounced upward-decreasing gamma-ray log trends, ranging in thickness from approximately 15 to 80 feet (sheet 1C). This log motif is common in progradational shallow marine systems (Van Wagoner and others, 1990). Petrographic data from three thin sections in core one provide detailed compositional data (sheet 1A). These samples are characterized as a laminated lithic siltstone (3,503 ft, mean grain size of 0.052 mm), a mudstone (3,514 ft), and a bioturbated, lithic lower very fine-grained sandstone (3,529 ft, mean grain size of 0.082 mm) (Pore Scale Solutions Ltd. and Santos Ltd., 2025). Framework grains (quartz, feldspar, carbonate, metamorphic, and plutonic rock fragments) comprise 50.5 percent and 47 percent, for the upper and lower non-mudstone samples, respectively. Ductile grains (intra- and extrabasinal rock fragments, micas, clays, and detrital organic matter) comprise 37.5 percent and 49.5 percent, respectively, with the remaining 12 percent and 3.5 percent, respectively, consisting of authigenic components (siderite, clays, and pyrite) (Pore Scale Solutions Ltd. and Santos Ltd., 2025).

Seismic Stratigraphy- Core one was recovered from a thick (~1,500 ft) succession of nearly horizontal, parallel topset seismic reflectors (figs. 3A, B). Topset reflectors are generally higher amplitude and more laterally continuous than the foreset and wedge reflectors associated with the underlying slope and transgressive wedge deposits.

Core Description- Core one consists nearly exclusively of massive to weakly bedded, bioturbated muddy and silty, very fine-grained sandstone (sheet 1A and B). In the isolated intervals where primary bedding is preserved, it consists of interbedded thinly to very thinly bedded mudstone and very fine-grained sandstone or contains thin mudstone laminae (figs. 8A–E). Small shell fragments are common throughout the core; however, one exceptionally well-preserved bivalve specimen was recovered at 3,506 ft md (fig. 8C). Dutro and Silberling (1988) reported fossils associated with the middle or late Albian *Gastroplites kingi* biostratigraphic zone in both cores one and three and identified taxa common to the upper part of the Torok and lower part of the Nanushuk formations. Recognizable trace fossils include *Planolites*, *Phycosiphon*, and possibly *Rhizocorallium* and *Teichichnus* (figs. 8B and E), constituents commonly associated with the *Cruziana* Ichnofacies (Seilacher, 1967).

Core Interpretation- The lack of preserved sedimentary structures precludes any detailed interpretation of hydrodynamic conditions present during the deposition of the sediments preserved in core one; however, the prevalence of intensely bioturbated interbedded fine-grained sandstone, silty sandstone, sandy mudstone, and mudstone, the presence of marine fossils, and occurrence within seismic topsets suggest deposition in a mixed- to low-energy marine environment. More specifically, lithologies and trace fossil assemblages indicate deposition within a low-energy middle to lower shoreface setting where sand is deposited and redistributed by fair weather and storm waves, and finer-grained, mud-rich intervals are the products of suspension deposition (MacEachern and Bann, 2008). The bioturbation index in core one is typically six (Taylor and Goldring, 1993), resulting in the nearly complete obliteration of the primary depositional fabric (sheet 1A and fig. 8). The seismic stratigraphy, gamma ray log profile, and depositional facies interpretations for this core indicate that it was recovered from the lower part of an approximately 60-ft-thick, shallowing-upwards, marine parasequence (Van Wagoner and others, 1990; sheet 1C).

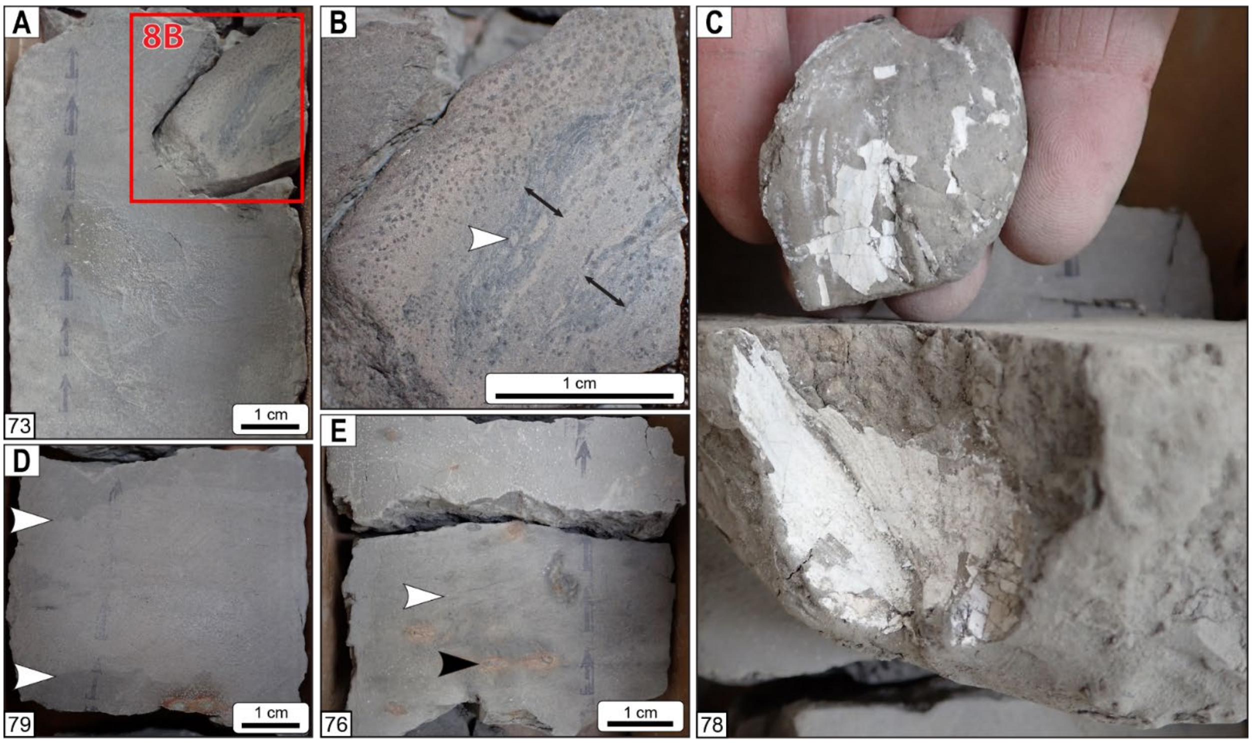

Figure 8. Detailed photographs of the Nanushuk Formation in core one. A. Massive silty, very fine-grained sandstone typical of core one. Red box indicates the location of figure 8B. B. Thin, bioturbated mudstone beds (black arrows) preserved in a concretion from core one containing *Planolites* burrows (white arrow). C. Bivalve recovered from 3,506 ft in core one. D. Irregular contacts (white arrows) between bioturbated, silty mudstone beds and very fine-grained silty sandstone bed. E. Discontinuous, wispy mudstone drapes (white arrow) and sideritized burrows (black arrow). The number in the lower-left corner refers to the photograph numbers, which are listed in the core description on sheet 1A. Cores are 2 inches wide.

Regional Petrology

Helmold and LePain (2021) proposed that sandstones of the Nanushuk Formation contain higher percentages of detrital carbonate grains in the northwestern part of their study area north of Umiat (fig. 1A) (mean of 5.2 percent), relative to locations in the southeastern part (mean of 0.3 percent). This regional compositional trend is related to carbonate-rich source lithologies of the western Brooks Range (fig. 1) and the Herald Arch, a basement-involved uplift beneath the western North Slope and southeastern Chukchi Sea (Grantz and others, 1975). Carbonate grains comprise 0.5–6.5 percent (mean of 3.3 percent) of framework grains in Nanushuk Formation samples from this well (Bartsch-Winkler, 1988; Pore Scale Solutions Ltd., and Santos Ltd., 2025), consistent with the geographic distribution of carbonate-rich Nanushuk Formation samples of Helmold and LePain (2021).

ACKNOWLEDGEMENTS

The interpretations presented in this report have benefited from technical discussions with Dave Houseknecht of the U.S. Geological Survey. A draft of this report was given a thoughtful review by Dave LePain, Marwan Wartes, Erin Campbell, and Kristen Janssen. Kurt Johnson, Kaleb Smith, and the GMC staff helped us access the cores, and we greatly appreciate their assistance.

REFERENCES

Alaska Oil and Gas Conservation Commissioner (AOGCC), 2014, J.W. Dalton and NPRA legacy well history report: Alaska Oil and Gas Conservation Commission, 600 p. File accessed May 4, 2023.

Bailey, A., 2016, A new oil resource: ConocoPhillips applies to AOGCC for rules for Kuparuk Moraine oil pool: Petroleum News, v. 21, no. 15, p. 1.

Bird, K.J., 2001, Framework geology, petroleum systems, and play concepts of the National Petroleum Reserve–Alaska, in Houseknecht, D.W., ed., NPRA core workshop: petroleum plays and systems in the National Petroleum Reserve–Alaska: SEPM Core Workshop no. 21, p. 5–18.

Bouma, A.H., 1962, Sedimentology of some flysch deposits, a graphic approach to facies interpretation: Elsevier, Amsterdam, 168 p.

Boyd, R., Dalrymple, R.W., and Zaitlin, B.A., 2006, Estuarine and incised-valley facies models, in Posamentier, H.W., and Walker, R.G., eds., Facies models revisited: SEPM Special Publication 84, 527 p.

Catuneanu, O., 2006, Principles of sequence stratigraphy: Amsterdam, Elsevier, 375 p.

Decker, P.L., 2010, Brookian sequence stratigraphic framework of the northern Colville foreland basin, central North Slope, Alaska (poster and presentation): DNR Spring Technical Review Meeting, Anchorage, April 21-22, 2010: Alaska Division of Geological & Geophysical Surveys, 30 p., 1 sheet. https://doi.org/10.14509/21861

Dumoulin, J.A., 2001, Lithologies of the basement complex (Devonian and older) in the National Petroleum Reserve–Alaska, in Houseknecht, D.W., ed., NPRA core workshop: petroleum plays and systems in the National Petroleum Reserve–Alaska: SEPM Core Workshop no. 21, p. 201–214.

Dutro, J.T., and Silberling, N.J., 1988, Megafossil biostratigraphy of some deep test wells, National Petroleum Reserve in Alaska, in Gryc, G., ed., Geology and exploration of the National Petroleum Reserve in Alaska, 1974–1982: U.S. Geological Survey Professional Paper 1399, p. 667–686.

Flemming, B.W., 2011, Geology, geomorphology, and sedimentology of estuaries and coasts, in Flemming, B.W., and Hansom, J.D., eds., Treatise on estuaries and coasts: Amsterdam, Elsevier, p. 7–38.

Gingras, M.K., MacEachern, J.A., and Dashtgard, S.H., 2011, Process ichnology and the elucidation of physico-chemical stress: Sedimentary Geology, v. 237, p. 115–134.

Goodbred, S.L., and Saito, Y., 2012, Tide-dominated deltas, in Davis, R.A., and Dalrymple, R.W., eds., Principles of tidal sedimentology: Springer Science + Business Media B.V., p. 129–149.

Grantz, A., Holmes, M.L., and Kesoski, B.A., 1975. Geologic framework of the Alaskan continental terrace in the Chukchi and Beaufort Seas. U.S. Geological Survey Open-file Report 75-124. 43 p.

Grantz, A., and May, S.D., 1982, Rifting history and structural development of the continental margin north of Alaska, in Watkins, J.S., and Drake, C.L., eds., Studies in continental margin geology: American Association of Petroleum Geologists Memoir no. 64, p. 77–100.

Grantz, A., May, S.D., and Hart, P.E., 1994, Geology of the Arctic continental margin of Alaska, in Plafker, G., and Berg, H.C., eds., The geology of Alaska: Geological Society of America, p. 17–48.

Haywood, H., and Legg, G.W., 1983, Geological report: J.W. Dalton Test Well No. 1: Prepared by Husky Oil NPR Operations, Inc., for the U.S. Geological Survey, 39 p.

Helmold, K.P., and LePain, D.L., 2021, Sedimentary petrology, reservoir quality, and provenance of Albian–Cenomanian Nanushuk Formation sandstone, NPRA test wells, Umiat 18, and measured outcrop sections, central North Slope, Alaska, in LePain, D.L., and Helmold, K.P., eds., Sedimentology and reservoir quality of the Nanushuk Formation (Albian-Cenomanian) in cores from the National Petroleum Reserve–Alaska and adjoining state lands to the south: Alaska Division of Geological & Geophysical Surveys Report of Investigation 2021-4B, 31 p. https://doi.org/10.14509/30728

Homza, T.X., 2004, A structural interpretation of the Fish Creek Slide (Lower Cretaceous), northern Alaska: American Association of Petroleum Geologists Bulletin, v. 88, no. 3, p. 265–278.

Homza, T.X., Fillerup, M.A., and Gardner, D.W., 2020, Toward a better understanding of northern Alaska's petroleum systems: deconstructing the Barrow Arch: American Association of Petroleum Geologists Bulletin, v. 104, no. 8, p. 1,793–1,816.

Houseknecht, D.W., 2019, Petroleum systems framework of significant new oil discoveries in a giant Cretaceous (Aptian–Cenomanian) clinothem in Arctic Alaska: American Association of Petroleum Geologists Bulletin, v. 103, no. 3, p. 619–652.

Houseknecht, D.W., and Bird, K.J., 2011, Geology and petroleum potential of the rifted margins of Arctic Alaska and the Chukchi borderland: AAPG Search and Discovery Article #10293, adapted from oral presentation at AAPG International Conference and Exhibition, Calgary, Canada, September 12–15, 2010.

Houseknecht, D.W., Bird, K.J., and Schenk, C.J., 2009, Seismic analysis of clinoform depositional sequences and shelf-margin trajectories in Lower Cretaceous (Albian) strata, Alaska North Slope: Basin Research, v. 21, p. 644–654.

Houseknecht, D.W., Lease, R.O., Schenk, C.J., Mercier, T.J., Rouse, W.A., Jarboe, P.J., Whidden, K.J., Garrity, C.P., Lewis, K.A., Heller, S.J., Craddock, W.H., Klett, T.K., Le, P.A., Tennyson, M.E., Gaswirth, S.B., Woodall, C.A., Brownfield, M.E., Leathers-Miller, H.M., and Finn, T.M., 2017, Assessment of undiscovered oil and gas resources in the Cretaceous Nanushuk and

Torok Formations, Alaska North Slope, and summary of resource potential of the National Petroleum Reserve in Alaska: U.S. Geological Survey Fact Sheet 2017-3088, 4 p.

Lease, R.O., Houseknecht, D.W., and Kylander-Clark, A.R.C., 2022, Quantifying large-scale continental shelf margin growth and dynamics across middle-Cretaceous Arctic Alaska with detrital zircon U-Pb dating: Geology, v. 50, no. 5, p. 620–625.

LePain, D.L., and Helmold, K.P., 2021, Core descriptions, sedimentology and reservoir potential of the Nanushuk Formation (Albian-Cenomanian), eastern National Petroleum Reserve-Alaska, in LePain, D.L., and Helmold, K.P., eds., Sedimentology and reservoir quality of the Nanushuk Formation (Albian-Cenomanian) in cores from the National Petroleum Reserve–Alaska and adjoining state lands to the south: Alaska Division of Geological & Geophysical Surveys Report of Investigation 2021-4A, 46 p., 6 sheets. https://doi.org/10.14509/30727

Longhitano, S.G., Mellere, D., Steel, R.J., and Ainsworth, R.B., 2012, Tidal depositional systems in the rock record: A review and new insights: Sedimentary Geology, v. 279, p. 2–22.

Lowe, D.R., 1982, Sediment gravity flows II: Depositional models with special reference to the deposits of high-density turbidity currents: Journal of Sedimentary Petrology, v. 52, no. 1, p. 279–297.

MacEachern, J.A., and Bann, K.L., 2008, The role of ichnology in refining shallow marine facies models, in Hampson, G.J., Steel, R.J., Burgess, P.M., and Dalrymple, R.W., eds., Recent advances in models of siliciclastic shallow-marine stratigraphy: SEPM Special Publication 90, p. 73–116.

Mickey, M.B., Haga, Hideyo, and Bird, K.J., 2006, Micropaleontology of selected wells and seismic shot holes, Northern Alaska: U.S. Geological Survey Open-File Report 2006-1055, 11 p.

Miller, J.J., Agena, W.F., Lee, M.W., Zihlman, F.N., Grow, J.A., Taylor, D.J., Killgore, Michele, and Oliver, H.L., 2000, Regional seismic lines reprocessed using post-stack processing techniques; National Petroleum Reserve, Alaska: U.S. Geological Survey Open-File Report 2000-286., https://pubs.usgs.gov/of/2000/ofr-00-0286/.

Molenaar, C.M., 1983, Depositional relations of Cretaceous and lower Tertiary rocks, northeastern Alaska: American Association of Petroleum Geologists Bulletin, v. 67, no. 7, p. 1066–1080.

Mull, C.G., 1985, Cretaceous tectonics, depositional cycles, and the Nanushuk Group, Brooks Range and Arctic Slope, Alaska, in Huffman, A.C., ed., Geology of the Nanushuk Group and related rocks, North Slope, Alaska: U.S. Geological Survey Bulletin 1614, p. 7–36.

Mull, C.G., Houseknecht, D.W., and Bird, K.J., 2003, Revised Cretaceous and Tertiary stratigraphic nomenclature in the Colville Basin, northern Alaska: U.S. Geological Survey Professional Paper 1673, 59 p.

Plink-Björklund, P., 2012, Effects of tides on deltaic deposition: Causes and responses: Sedimentary Geology, v. 279, p. 107–133.

Pore Scale Solutions Ltd., and Santos Ltd., 2025, Petrographic analysis of Nanushuk Formation samples from the Barrow, East Simpson, East Topagoruk, Fish Creek, J. W. Dalton, Kaolak, Meade, Oumalik, South Meade, Topagoruk, Tunalik, and Tungak Creek wells in the National

Petroleum Reserve in Alaska (NPR-A): Alaska Division of Geological & Geophysical Surveys Geologic Materials Center Data Report 471, 136 p. https://doi.org/10.14509/31742

Posamentier, H.W., and Allen, G.P., 1993, Variability of the sequence stratigraphic model: effects of local basin factors: Sedimentary Geology, v. 86, p. 91–109.

Reineck, H.E., and Singh, I.B., 1973, Depositional Sedimentary Environments: New York, Springer, 549 p.

Reineck, H.E., and Wunderlich, F., 1968, Classification and origin of flaser and lenticular bedding: Sedimentology, v. 11, p. 99–104.

Reynaud, J.Y., and Dalrymple, R.W., 2012, Shallow-marine tidal deposits, in Davis, R.A., and Dalrymple, R.W., eds., Principles of tidal sedimentology: Springer Science+Business Media B.V., p. 335–369.

Ruppert, N.A., Jadamec, M.A., Freymueller, J.T., Rollins, C., Freymueller, J.T., Xue, X., Holtkamp, S.G., Logan, T.A., Meyer, F., and Patton, J., 2024, The 2018 Kaktovik, Alaska earthquakes and their context: insights from seismotectonics, InSAR geodesy, and static stress changes, in Ruppert, N.A., Jadamec, M.A., and Freymueller, J.T., eds., Tectonics and seismic structure of Alaska and northwestern Canada: https://doi.org/10.1002/9781394195947.ch22.

Seilacher, A., 1967, Bathymetry of trace fossils: Marine Geology, v. 5, p. 413–428.

Sommer, J.V., Dorrington, K., VanDenburg, C., Bonelli, J.R., and Alonso, J.L.A., 2021, Pikka field and the opening of the Nanushuk play, North Slope, Alaska, in Sternbach, M.R.K., and Dolson, J.C., eds., Giant fields of the decade: 2010–2020: American Association of Petroleum Geologists Memoir 125, p. 301–338.

Taylor, A.M., and Goldring, R., 1993, Description and analysis of bioturbation and ichnofabric: Journal of the Geological Society (London), v. 150, p. 141–148.

Van Wagoner, J.C., Mitchum, R.M., Campion, K.M., and Rahmanian, V.D., 1990, Siliciclastic sequence stratigraphy in well logs, cores, and outcrops: Concepts for high-resolution correlation of time and facies: American Association of Petroleum Geologists Methods in Exploration Series no. 7, 55 p.

Weimer, P., 1987, Seismic stratigraphy of three areas of lower slope failure, Torok Formation, northern Alaska, in Tailleur, I.L., and Weimer, P., eds., Alaskan North Slope geology: Anchorage, Alaska, Alaska Geological Society, p. 481–496.

Zihlman, F.N., and Oliver, H.L., 1999, Selected data from eleven wildcat wells in the National Petroleum Reserve in Alaska: U.S. Geological Survey Open-File Report 99-015.